Kinetics and Molar Mass Evolution during Atom Transfer Radical Polymerization of *n*-Butyl Acrylate Using Automatic Continuous Online Monitoring

Emmanuel Mignard,[†] Jean-François Lutz,[‡] Thierry Leblanc,[§] Krzysztof Matyjaszewski,[⊥] Olivier Guerret,[∥] and Wayne F. Reed*[,§]

CNRS UMR6509, Université de Rennes 1-Campus de Beaulieu, 35042 Rennes Cedex, France, Fraunhofer Institute For Applied Polymer Research, 14476 Potsdam, Germany, Department of Physics, Tulane University, New Orleans, Louisiana 70118, Chemistry Department, Carnegie Mellon University, Pittsburgh, Pennsylvania 15213, and Arkema, Groupement de Recherche de Lacq, 64170 Lacq, France

Received March 21, 2005; Revised Manuscript Received June 15, 2005

ABSTRACT: Homogeneous bulk atom transfer radical polymerization (ATRP) of *n*-butyl acrylate (BA) was monitored by automatic continuous online monitoring of polymerization reactions (ACOMP). This allowed simultaneous monitoring of conversion, weight-average molar mass M_w, and intrinsic viscosity, from which the viscometric average molar mass M_v, and an index of polydispersity M_w/M_v, were also determined. For ATRP of BA, initiated by methyl 2-bromopropionate and catalyzed by copper bromide complexes with 4,4′-di(5-nonyl)-2,2′-bipyridine, ACOMP yielded an equilibrium constant, $K_{eq}(90\ °C) = 5.8 \times 10^{-10}$. The polymerizations exhibited first-order kinetics with respect to monomer and initiator concentrations, as expected for ATRP. These results set the stage for further detailed understanding of kinetics and mechanisms in ATRP reactions using ACOMP, where temperature and concentration dependences can be readily monitored.

Introduction

Controlled radical polymerization (CRP) is a powerful technique for macromolecular engineering, allowing control of molecular weight, polydispersity, functionality, copolymer composition, and architecture.[1−4] Among the reported means for CRP is atom transfer radical polymerization (ATRP), nitroxide mediated polymerization (NMP), and reversible addition fragmentation transfer polymerization (RAFT). An extensive literature on CRP exists, much of which has been recently reviewed.[5−8]

In this report the focus is on ATRP.[7−9] Scheme 1 gives the key equilibrium between activated and deactivated species (respectively $P_n^{\bullet}$ and P_n−X). In the presence of monomer M, only a small fraction (≪1%) of activated species can propagate until they are deactivated via the halogen atom transfer reaction. This means there is a repeated growth cycle for every chain. If the reversible activation occurs frequently enough over a period of polymerization time, every deactivated chain will have a nearly equal chance to grow, with a result similar to living ionic polymerization. This control allows a targeted molecular weight (up to ∼100 kg/mol) with low polydispersity index (near 1.1) to be obtained.

Harnessing the full potential of ATRP requires detailed understanding of kinetics and mechanisms.[10,11] Several kinetic studies were already reported,[11] virtually all of which use discrete sampling techniques, in which aliquots were withdrawn at intervals during conversion, and analyzed afterward.[12−17] Frequently used techniques include size exclusion chromatography (SEC), NMR, gas chromatography (GC), gravimetry, electron spin resonance (ESR), and matrix assisted laser desorption ionization Time-of-Flight (MALDI−TOF) mass spectroscopy. However, one of the key requirements to fully control the synthesis of such well-defined materials is to monitor the chemistry (i.e., kinetics, molecular weight, chemical composition, etc.) during the synthesis. From the information obtained in quasi-real time it should be possible to act upon the material synthesis or design by adding a comonomer or a grafting agent at the right time. Moreover, it may be possible to correct the process if the reaction begins to fail. Perhaps the only continuous method currently used in monitoring ATRP involves empirically based near infrared (NIR) measurements, which is limited primarily to determining monomer conversion.[18]

Scheme 1. General Scheme for ATRP

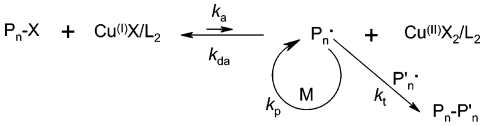

Automatic continuous online monitoring of polymerization reaction (ACOMP) was recently introduced.[19,20] It is not a chromatographic analysis, and there is no injection of a withdrawn sample. Rather, signals (e.g., light scattering, viscosity, differential refractive index, and UV−visible absorption in this work) are obtained from a continuously diluted reactor stream and combined in a model-independent fashion. It is thus possible to follow simultaneously and in near real time absolute weight-average molar mass M_w, weight-average intrinsic viscosity $[\eta]_w$, monomer and polymer concentrations, and monomer conversion, including the case of copolymerization.[21] In addition, certain indices of polydispersity can be determined.[22] Hence, ACOMP permits absolute characterization of polymers during the synthesis.

* Corresponding author. E-mail: wreed@tulane.edu.
[†] Université de Rennes 1-Campus de Beaulieu.
[‡] Fraunhofer Institute for Applied Polymer Research.
[§] Tulane University.
[⊥] Carnegie Mellon University.
[∥] Arkema, Groupement de Recherche de Lacq.

10.1021/ma050590r CCC: $30.25
Published on Web 10/18/2005

Table 1. Experimental Conditions for Bulk ATRP Reactions Followed by ACOMP

	BA/Cu^{I}/dNbpy/Cu^{II}/M2BP molar ratios	BA (mL)	$Cu^{I}Br$ (g)	dNbpy (g)	$Cu^{II}Br_2$ (g)	vol fraction[a]	M2BP (g)[b]	baseline time (s)	temp (°C)
a	175/0.9/1.7/0/1	25	0.125	0.709	0	0.075	0.147	1345	90
b	165/0.8/1.7/0.04/1	30	0.149	0.894	0.012	0.075	0.176	2206	90
c	210/1/2.1/0.025/1	30	0.150	0.866	0.006	0.025	0.160	2009	90
d	200/1/2.1/0.05/1	30	0.150	0.877	0.012	0.025	0.169	2053	90
e	100/0.5/1/0/1	20	0.104	0.604	0	0.025	0.206	2237	90
f	200/1/2/0/1	25	0.125	0.745	0	0.025	0.139	2025	90
g	500/2.5/5/0/1	30	0.150	0.856	0	0.025	0.067	2011	90
h	1000/5/10/0/1	50	0.250	1.426	0	0.025	0.057	2026	90
i	200/1/2/0/1	50	0.251	1.426	0	0.025	0.283	1855	70
j	200/1/2/0/1	25	0.125	0.744	0	0.025	0.138	2000	80

[a] Total flow rate of both pumps was set to 2 mL/min. [b] Initiator was injected after withdrawing a volume of reaction solution corresponding to the time of the monomer baseline, taking into account the volume fraction of reactor fluid present in the diluted solution flowing through the detector train. Normalized time t_0 of the polymerization corresponds to the injection of the initiator into the reactor, which means right after acquiring the baseline time.

Table 2. Monomer, Polymer, and Copper Complexes Properties in Solution in THF

	$(\partial n/\partial c Z)$ (mL/g)	A_2 (mL·mol/g^2)	density (g/mL)	(dV/dc) at 699 nm (V·mL/g)[a]	abs coeff (L/mol/cm)
BA	0.0148	NA	0.894	NA	NA
PBA	0.0615	0.000 88	1.087	NA	NA
$Cu^{I}Br/dNbpy_2$	0.602[a]	NA	NA	118	8.6
cationic form of $Cu^{II}Br_2/dNbpy_2$	1.535[a]	NA	NA	2652	296

[a] g of copper bromide only. NA: Not Applicable.

Thus, it is of keen interest to apply ACOMP to CRP. A first study of bulk NMP of *n*-butyl acrylate (BA) was recently published.[23] Another study involving bulk nitroxide mediated gradient copolymerization of BA with styrene also gave the composition profile of macromolecules and allowed the determination of sequence length averages, reactivity ratios, copolymer static and hydrodynamic dimensions, and molecular weights.[24] These encouraging results on NMP have stimulated the present work on ATRP. However, using ACOMP for monitoring ATRP is more challenging than for NMP since ATRP requires the use of transition metal catalysts, which can have limited solubility and can be oxidized and, consequently, complicates the analytical procedures.

Here, the first ACOMP analysis of a bulk ATRP of BA is reported. BA was chosen as a model monomer since (i) this monomer is industrially important, (ii) it possesses a very low glass transition temperature (T_g) and therefore bulk polymerization can be potentially monitored up to moderate monomer conversion, (iii) the combination of copper(I) bromide ($Cu^{I}Br$) with the ligand 4,4′-di(5-nonyl)-2,2′-bipyridine (dNbpy) was previously reported to be efficient for controlling such polymerization,[15] (iv) the ATRP kinetics of BA were previously studied via standard aliquot methods and therefore the results of the present paper can be compared to previous studies[15,25−28] and (v) the bulk ATRP of BA in the presence of CuBr and dNbipy seems to be homogeneous.[15]

Materials and Methods

Reagents. Copper(I) bromide (Aldrich, 99.999%) was washed with glacial acetic acid to remove the soluble fraction of Cu(II) species, filtered, washed with absolute ethanol and diethyl ether, and dried by vacuum. BA (Aldrich 99%) was filtered on an alumina column to remove traces of inhibitor (monomethyl ether hydroquinone), and then deoxygenated by nitrogen flush prior to use. Copper(II) bromide (Aldrich, 99.999%) and methyl 2-bromopropionate (M2BP) (Aldrich, 98%) were used as received. 4,4′-Di-(5-nonyl)-2,2′-bipyridine (dNbpy) was synthesized and purified as described previously.[13]

Sequence of Operations during ATRP Monitoring. Copper(I) bromide, dNbpy (and optionally copper(II) bromide) were added to a dry Schlenk flask, as given in Table 1. The flask was thoroughly purged by a vacuum for 1 h. Then deoxygenated BA was added into the reactor via a degassed syringe through a septum. The mixture was stirred for 30 min to preform the copper-based complexes. Then, the flask was transferred to a thermostated oil bath and was connected to the ACOMP system. The reactor was preheated while the baseline of the ACOMP dilution solvent (THF) was acquired. Then, the reaction mixture was pumped and diluted to obtain the monomer baseline acquisition, during which the M2BP initiator was purged by nitrogen and then was added via a degassed syringe into the reactor. The time t_0 of the experiment corresponds to the injection of the initiator into the reactor. At the end of the polymerization, the ACOMP system was cleaned with THF and the reaction mixture was filtered on neutral alumina column in order to remove copper-based complexes, and the polymer was recovered by heating the solution under vacuum at 50 °C.

ACOMP Instrumentation and Method. ACOMP methods and instrumentation have been described in detail elsewhere.[19−24] Briefly, a small sample stream was pumped from the reactor at a constant rate and continuously mixed with a much larger flow of solvent. The dilution solvent (THF) was purged by nitrogen prior to use and during the entire experiment in order to avoid oxidation of catalysts. In the experiments the high pressure-mixing scheme used for the original CRP monitoring was used, involving two Agilent 1100 HPLC pumps with an Upchurch microbore-mixing chamber at their outlet. The diluted stream passed through a series of detectors, including a home-built multiangle light scattering unit,[29] and capillary viscometer,[30] a Shimadzu SPD-10AV spectrophotometer, and a Waters 410 refractometer (RI). The reactor temperature was monitored via a K-type thermocouple. All of the instrument outputs were led through a 12 bit A/D converter (Data Translation 2801) to a computer. Data gathering and analysis software were written in house.

Figure 1 shows raw data obtained from a typical ACOMP monitored ATRP experiment: 25 mL of BA with molar ratios BA/ligand/Cu(I)/initiator: 200/2/1/1, at 90 °C, under nitrogen atmosphere, and no added Cu(II) as reported in Table 1 (experiment f). From $t = 0$ to 1025s only THF flows through the detectors, after which 2.5% of monomer with the Cu(I)/ligand mixture in THF flows. Initiator was added at 2410 s. The polymerization reaction is reflected in the three detector

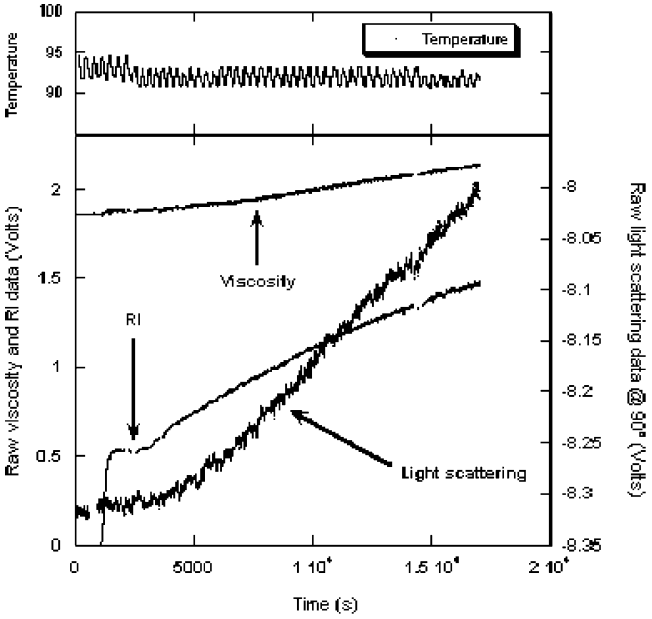

Figure 1. Raw ACOMP data for a typical ATRP experiment, i.e., 0.894 g/mL of BA with molar ratios BA/Cu(I)/ligand/initiator: 200/1/2/1, at 90 °C under nitrogen atmosphere (experiment f in Table 1).

signals shown after 650 s. This delay time depends only on flow rate and plumbing. The viscosity and 90° light scattering data show the increase in polymer molecular mass and concentration, whereas the increase in the index of refraction shows conversion, according to the differential refractive index ($\partial n/\partial c$) of BA and poly(*n*-butyl acrylate) (PBA) in THF. Figure 1 also shows reactor temperature.

Table 2 gives a summary of optical and other properties of BA, PBA, and $Cu^{I}Br$ and $Cu^{II}Br_2$ based complexes. The second virial coefficient A_2 of PBA in THF and both $\partial n/\partial c$ of BA and PBA used in this work were determined by Chauvin et al.[23] $\partial n/\partial c$ computations were performed according to the method of Brousseau et al.[31] and, for the range of molecular weights monitored in this study (i.e., > 5000 g/mol), the $(\partial n/\partial c)_{PBA}$ can be considered as a constant.

The methods of combining the detector signals to obtain concentrations, M_w, $[\eta]$, and M_w/M_v, have been detailed in earlier work,[19−24] and they include reactor density corrections[23] and the use of the Zimm approximation for light scattering.[32]

Viscometric average molecular mass, M_v, was computed according to the Mark−Houwink−Sakurada equation, with the following prefactor and exponent.[23]

$$[\eta] = 0.00927 M_v^{0.737} \quad (1)$$

The use of the spectrophotometer at 699 nm in order to determine Cu(I) and Cu(II) concentrations is novel to this work. It was shown in previous works that both $Cu^{I}Br/dNbpy_2$ activator and $Cu^{II}Br_2/dNbpy_2$ deactivator absorb in the visible range.[33,34] $Cu^{II}Br_2/dNbpy_2$ has an absorption band whose maximum is located between 650 and 750 nm. $Cu^{I}Br/dNbpy_2$ also absorbs in that range but with a smaller absorption coefficient (ϵ). In low polar media such as BA and in the presence of an excess of Cu(I) activator, $Cu^{II}Br_2/dNbpy_2$ complexes mostly exist under a trigonal bipyramidal cationic form $[Cu(II)-(dNbpy)_2Br]^+,[Br]^-$.[33] Hence, it was assumed that the monitored signal was only due to the active forms of each copper-based complexes that are able to establish the equilibrium between activated and deactivated species, i.e., $Cu^{I}Br/dNbpy_2$ activator and cationic $Cu^{II}Br_2/dNbpy_2$ deactivator (cf. Scheme 1).

Two ACOMP experiments were used to calibrate the visible absorption. First, experiment **a** was done without added $Cu^{II}Br_2$ prior to injection of the initiator (cf. Table 1) to obtain the detector response $(dV/dc)_{Cu^{I}Br}$. Raw RI and 699 nm data are plotted in Figure 2. When monitoring of the reaction mixture baseline began the 699 nm signal jumped to a fixed value (at 615 s), corresponding to the absorption of $Cu^{I}Br$ based complex only, and remained constant until the initiator was added. After initiation at 1960s the 699 nm signal shows the increase of Cu(II) concentration as a result of the decrease of $Cu^{I}Br$ concentration, since the former has a larger ϵ. Indeed, the halogen transfer between initiator and $Cu^{I}Br$ as seen in Scheme 1 leads to the formation of cationic form of $Cu^{II}Br_2$ and also radical that can initiate the polymerization reaction. A similar experiment was carried out with initially added $Cu^{II}Br_2$ at 5 mol % vs $Cu^{I}Br$ (experiment b in Table 1) to obtain the detector response $(dV/dc)_{Cu^{I}Br}$ at 699 nm.

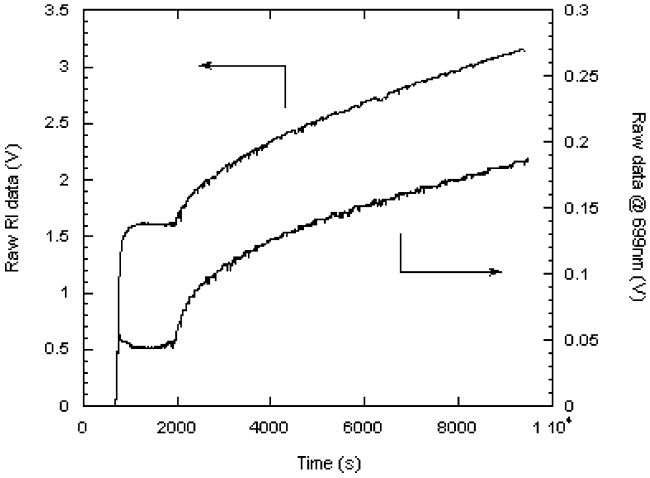

Figure 2. Raw ACOMP data obtained from the RI detector and at 699 nm for experiment a in Table 1.

$$V_{Vis}(t) = \left(\frac{dV}{dc}\right)_{Cu^{I}Br} c_{Cu^{I}Br} + \left(\frac{dV}{dc}\right)_{Cu^{II}Br_2} c_{Cu^{II}Br_2} \quad (2)$$

In this work, c_x means the mass concentration of x in the detector train (g/mL) while C_x means mass concentration in the reactor (also in g/mL). Molar concentrations in the reactor are denoted as usual, i.e., $[x]$. $[x]_0$, $C_{x,0}$ or $c_{x,0}$ means concentration of x at t_0. The ratio c_x/C_x is equal to the volume fraction of reactor fluid present in the diluted solution flowing through the detector train (cf. Table 1).

The absorption coefficients obtained from the above method are reported in Table 2. Calculated ϵ of the cationic $Cu^{II}Br_2/dNbpy_2$ in THF is in good agreement with the previously reported value.[34]

$\partial n/\partial c$ of both copper complexes was obtained from the RI detector signal by

$$V_{RI}(t) = K\left[\left(\frac{\partial n}{\partial c}\right)_{BA} c_{BA} + \left(\frac{\partial n}{\partial c}\right)_{PBA} c_{PBA} + \left(\frac{\partial n}{\partial c}\right)_{Cu^{I}Br} c_{Cu^{I}Br} + \left(\frac{\partial n}{\partial c}\right)_{Cu^{II}Br_2} c_{Cu^{II}Br_2}\right] \quad (3)$$

Here K is the RI calibration factor in terms of refractive index unit per Volt. $\partial n/\partial c$ of $Cu^{I}Br$ was computed with experiment **a** since there was no polymer nor $Cu^{II}Br_2$ during the baseline monitoring. $(\partial n/\partial c)_{Cu^{II}Br_2}$ was calculated from the baseline obtained with experiment b. Results are reported in Table 2.

Size Exclusion Chromatography (SEC). The final reaction products were cross-checked independently with SEC, using both traditional column calibration with polystyrene standards, and a seven angle light scattering detector, a Brookhaven Instruments Corp. BI-MwA (Holtsville, NY) connected to a Shimadzu RID-10A refractometer. This SEC system comprised an Agilent 1100 isocratic pump, Polymer Labs 10 μm Mixed B column, and THF was used at a flow rate of 1.0 mL/min.

Results and Discussion

ACOMP Monitoring of Monomer and Polymer Concentrations. Figure 3 shows the semilogarithmic

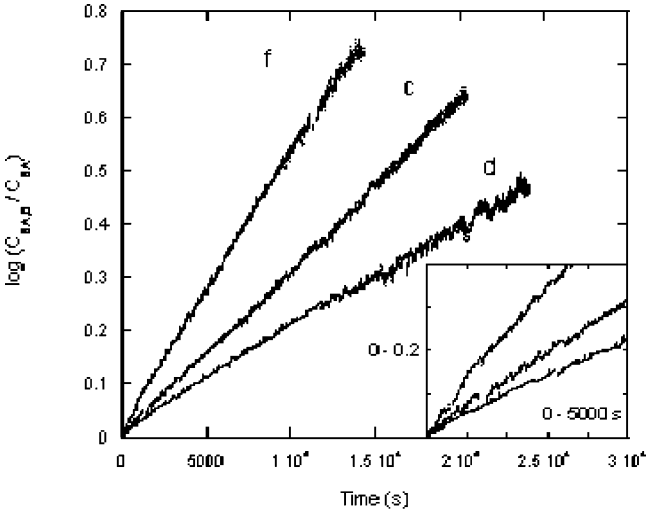

Figure 3. Semilogarithmic kinetic plots for experiments with variable concentration of $Cu^{II}Br_2$ added prior initiator injection, from top to bottom: 0 (experiment f), 0.025 (experiment c) and 0.05 equiv vs $Cu^{I}Br$ (experiment d) at 90 °C. The lower inset shows close up of the early stage of the BA ATRP reactions. Time is normalized.

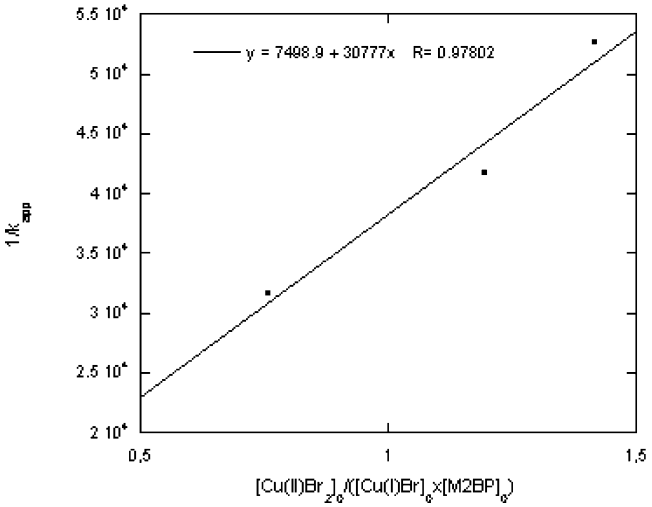

Figure 4. Determination of K_{eq} according to eq 5. The experimental points correspond to experiments b, c, and d of Table 1.

plots of the conversion of butyl acrylate $\log(C_{BA,0}/C_{BA})$ as a function of time, measured by ACOMP for three different ATRP experiments (experiments c, d, and f of Table 1) started in the presence of various initial concentrations of the deactivator $Cu^{II}Br_2$. The rate of the reaction dramatically decreased with increasing initial amounts of $Cu^{II}Br_2$. The latter is expected in ATRP kinetics since an initial excess of ATRP deactivator (i.e., $Cu^{II}Br_2$) shifts the equilibrium toward dormant species and reduces the concentration of propagating free radicals (Scheme 1). Nevertheless, the shape of the semilogarithmic plots was found to be slightly different in the presence and in the absence of initial deactivator. For the experiment started in the absence of additional deactivator (experiment f), in the early stages of the polymerization a downward curvature was observed (see inset Figure 3), whereas in the presence of initial deactivator (experiments c and d) linear plots were observed. This is a consequence of the persistent radical effect (PRE). ATRP reactions are subject to the persistent radical effect as first described theoretically by Hanns Fischer.[35,36] In ATRP, the deactivator ($Cu^{II}X_2/L_2$ in Scheme 1) is a persistent species which can only react with the transient propagating radicals $P_n^{\bullet}$, whereas the latter can also be consumed by self-combination. Therefore, during the polymerization, $[P_n^{\bullet}]$ decreases continuously while $[Cu^{II}X_2/L_2]$ increases.[35,36] This particular behavior results in unique kinetic trends, which differ from the steady state kinetics commonly observed for conventional radical polymerizations.[11,35,36]

Table 3. Kinetic Results from ACOMP Experiments

	BA/$Cu^{I}Br$/dNbpy/$Cu^{II}Br_2$/M2BP molar ratios	temp (°C)	k_{app} (s^{-1})	[P°] (mol L^{-1})
a	175/0.9/1.7/0/1	90	3.55×10^{-5}	6.28×10^{-10}
b	165/0.8/1.7/0.04/1	90	2.40×10^{-5}	4.25×10^{-10}
c	210/1/2.1/0.025/1	90	3.16×10^{-5}	5.59×10^{-10}
d	200/1/2.1/0.05/1	90	1.90×10^{-5}	3.36×10^{-10}
e	100/0.5/1/0/1	90	7.22×10^{-5}	1.28×10^{-9}
f	200/1/2/0/1	90	5.14×10^{-5}	9.10×10^{-10}
g	500/2.5/5/0/1	90	1.85×10^{-5}	3.27×10^{-10}
h	1000/5/10/0/1	90	5.74×10^{-6}	1.02×10^{-10}
i	200/1/2/0/1	70	9.77×10^{-6}	2.42×10^{-10}
j	200/1/2/0/1	80	3.51×10^{-5}	7.31×10^{-10}

Table 4. Set of Different Values of the Equilibrium Constant Obtain for the ATRP of BA

temp (°C)	ligand	solvent	K_{eq}	reference
110	dHbipy[a]	*p*-xylene	6.25×10^{-10}	27
110	dHbipy[a]	butyl acetate	7.80×10^{-10}	27
90	dNbipy	bulk	5.80×10^{-10}	this work
90	dNbipy	bulk	4.00×10^{-10}	28

[a] dHbipy: 4,4′-di-*n*-heptyl-2−2′-bipyridine.

In the absence of initial deactivator semilogarithmic plots of monomer conversion with time should theoretically be nonlinear. This was clearly experimentally observed in nitroxide mediated polymerization.[37,38] On the other hand, in most ATRPs, the kinetic features of the PRE may be experimentally masked by factors, which are not taken into account in the theory such as the presence of a low initial amount of deactivator (e.g., coming from slightly oxidized activator) or a chain length dependence of the termination step.[39−43] The typical downward curvature due to the PRE can be only observed if the reagents (particularly the activator) are carefully purified prior to experiment and if a very careful kinetic monitoring is done.[40,42,43]

The ACOMP results of Figure 3 allow visualization of the PRE kinetics at the early polymerization stages. The typical downward curvature observed for the experiment started in the absence of additional deactivator is due to the PRE. More precisely, three kinetic phases theoretically take place when the reaction mixture do not contain any initial $Cu^{II}Br_2$. The first phase is very short (hence difficult to detect in such graphs) and corresponds to an initial regime, where the concentration of deactivator is still too low for controlling the reaction.[35,36] During that phase, transient radicals continuously undergo bimolecular terminations, leading to a decrease in their concentration, whereas $Cu^{II}Br_2$ concentration continuously increases. When the concentration of Cu(II) deactivator reaches a sufficient excess as compared to transient radicals, the activation−deactivation ATRP equilibrium (Scheme 1) takes place and the reaction is controlled. This second regime corresponds to the observed downward curvature. Nevertheless, at higher conversions (typically above 15% of BA conversion) the curvature characteristic of the PRE is no longer observable due to the chain length dependence of the termination step, thus a third "steady state"

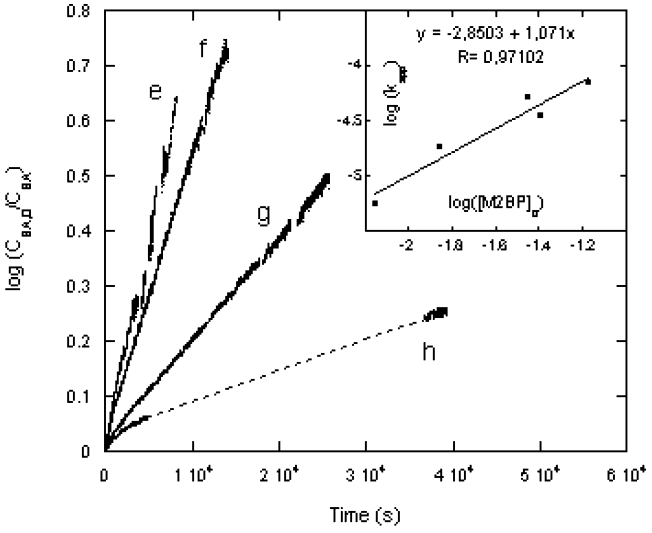

Figure 5. Semilogarithmic kinetic plots for experiments with different targeted degree of polymerization, from top to bottom: 100 (experiment e), 200 (experiment f), 500 (experiment g), and 1000 (experiment h). No $Cu^{II}Br_2$ was added prior initiator injection. From 5000 to 37000 s, data are missing for experiment h. However, we assume that the increase of $\log(C_{BA,0}/C_{BA})$ vs time should be constant between the two experimental points. The inset shows reaction order for the initiator at 90 °C (experiments a, e, f, g, and h): $[BA]_0 = 6.97$ M; $[Cu^IBr]_0 = [dNbpy]_0/2 = 0.035$ M. t_0 is set to 0.

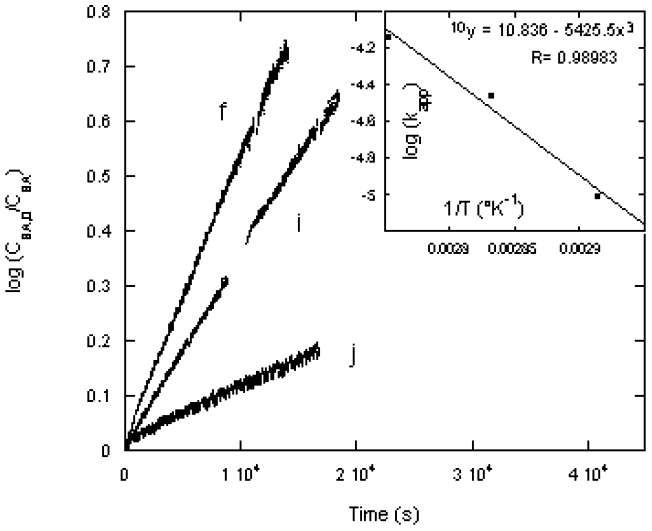

Figure 6. Semilogarithmic kinetic plots for experiments at different temperature, from top to bottom: 90 (experiment f), 80 (experiment i), and 70 °C (experiment j). No $Cu^{II}Br_2$ was added prior to initiator injection. The inset shows the temperature dependence plot for M2BP/Cu^IBr-mediated ATRP of BA (experiments f, i, and j): $[BA]_0 = 6.97$ M; $[Cu^IBr]_0 = [M2BP]_0 = [dNbpy]_0/2 = 0.035$ M. t_0 is set to 0.

regime is observed.[37,40,42] In contrast, for the reactions containing initially added $Cu^{II}Br_2$ (experiments c and d), the first phase is absent since a sufficient deactivator concentration is already available at time zero for controlling the reaction.[40] Thus, only an apparent steady-state regime was observed for these experiments (i.e., semilogarithmic plots are linear, which indicates first-order BA conversion and that the concentration of propagating radicals was constant throughout the polymerization).

Under these conditions (i.e., in the presence of initially added deactivator), the rate law for ATRP is described by eq 4.

$$\log\left(\frac{C_{BA,0}}{C_{BA}}\right) = k_p K_{eq}\frac{[Cu^IBr]}{[Cu^{II}Br_2]}[M2BP] \times t = k_p[P_n^\bullet] \times t = k_{app} \times t \quad (4)$$

Here, k_p is the absolute rate constant of polymerization, k_{app} is the apparent rate constant, and K_{eq} is the equilibrium constant between active and dormant species (Scheme 1). Thus, the experiments with added $Cu^{II}Br_2$ can be used for calculating K_{eq}. The latter is possible by plotting the reciprocal apparent rate constant as a function of $[Cu^{II}Br_2]_0/([Cu^IBr]_0[M2BP]_0$ and using

$$\frac{1}{k_{app}} = \frac{1}{k_p K_{eq}} \times \frac{[Cu^{II}Br_2]_0}{[Cu^IBr]_0[M2BP]_0} \quad (5)$$

Figure 4 shows $1/k_{app}$ as a function of $[Cu^{II}Br_2]_0/([Cu^IBr]_0[M2BP]_0$ for the experiments of Table 1 started in the presence of $Cu^{II}Br_2$ (i.e., experiments b, c, and d). In each case, k_{app} was calculated according to eq 5 (Table 3). The BA propagation rate constant k_p found from previous literature data was 56.5×10^3 L·mol^{-1}·s^{-1} at 90 °C.[44] The calculated slope in Figure 4 is 8.89×10^5 s^{-1}, yielding K_{eq} (90 °C) $= 5.8 \times 10^{-10}$. This number is in agreement with previously reported values shown in Table 4. Under similar experimental conditions (bulk, similar temperature, similar catalyst), Pyun et al. calculated K_{eq}(90 °C) $= 4 \times 10^{-10}$, using a kinetic approach based on a classic aliquots procedure.[28] The value calculated here is lower than the values found by Klumperman et al. at a higher temperature (Table 4),[27] since the ATRP equilibrium should be shifted toward the active species with increasing temperature.

Figure 5 shows semilogarithmic plots of BA conversion vs time for a series of experiments with different initial ratio monomer/initiator (i.e., different targeted degree of polymerization DP). The rate of polymerization decreases with the initial concentration of initiator $[M2BP]_0$, since the concentration of propagating radicals is directly related to the initial concentration of initiator. The inset to Figure 5 shows $\log(k_{app})$ vs $\log([M2BP]_0)$, indicating that the rate of polymerization is approximately linear with respect to the concentration of initiator. Figure 6 shows how the polymerization rate

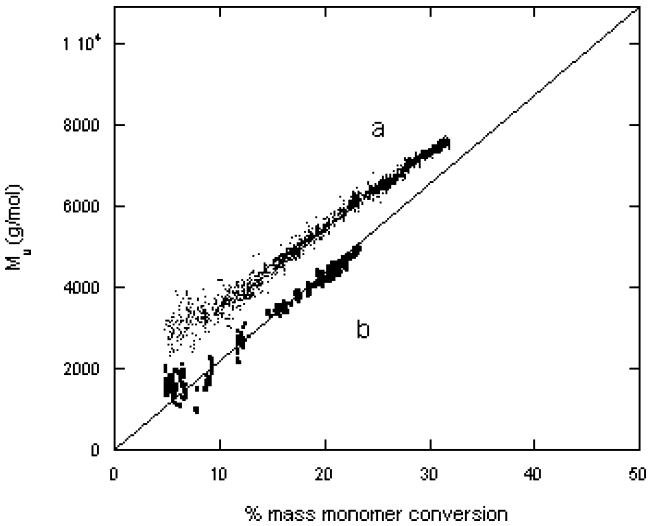

Figure 7. M_n vs mass monomer conversion for experiments a (small dots) and b (large dots). The diagonal line shows evolution of theoretical molecular weight.

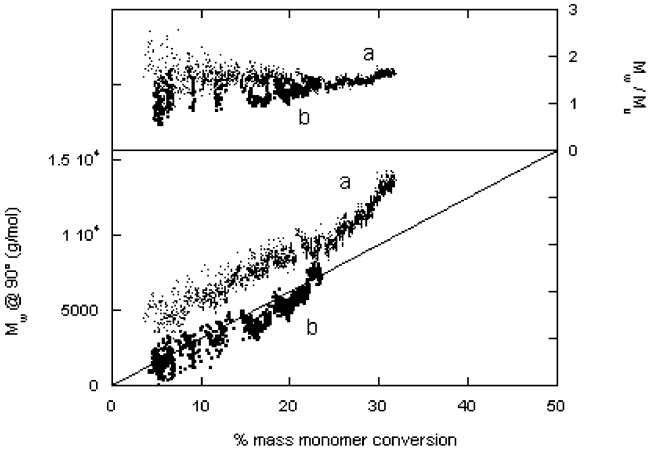

Figure 8. M_w (bottom) and M_w/M_v (top) vs mass monomer conversion for experiments a (small dots) and b (large dots). The diagonal lines show evolution of theoretical molecular weight assuming a constant polydispersity through the polymerization (about 1.2).

decreases with temperature. The latter additionally confirms that the activation−deactivation equilibrium is shifted toward dormant species when temperature is decreased. The slope of $\log(k_{app})$ vs $1/T$ (inset to Figure 6) is −5425.5, which corresponds to an apparent activation enthalpy ($\Delta H^{\ddagger}_{app}$) of 10.9 kcal·mol^{-1}. From the literature the activation enthalpy for BA propagation is $\Delta H^{\ddagger}_{prop}$ = 4.2 kcal·mol^{-1}.[44,45] Since the enthalpy of the preequilibrium is related to these last enthalpies, $\Delta H° = \Delta H^{\ddagger}_{app} - \Delta H^{\ddagger}_{prop}$, it is possible to calculate $\Delta H°$ = 6.7 kcal·mol^{-1}, which is close to values usually obtained with other ATRP systems: styrene/1-phenylethyl bromide or chloride/Cu^{I}Br or Cu^{I}Cl/dHeptylbpy: $\Delta H°$ = 4.8 and 6.3 kcal·mol^{-1} respectively;[13] methyl methacrylate/*p*-toluenesulfonyl chloride/Cu^{I}Cl/dNbpy: $\Delta H°$ = 9.7 kcal·mol^{-1}.[14]

ACOMP Determination of Reduced Viscosity and Molecular Weights. Figure 7, shows M_v vs mass monomer conversion for experiments a and b. Both plots of M_v show a linear increase in molecular weight, very close to the theoretical expectation consistent with the ATRP mechanism. The bottom panel of Figure 8 shows M_w vs monomer conversion for experiments a and b.[46] The top panel shows the ratio M_w/M_v, which is comprised between 1.6 and 1.1. Although the ratio M_w/M_v is not the polydispersity index commonly used, it provides a useful indication of the polydispersity, since M_v is very close to M_n for such a controlled mechanism.

For all the experiments, Table 5 reports conversion and theoretical M_n obtained at the end of the monitoring, and also the final values of M_w and M_v calculated by ACOMP as well as M_w and M_w/M_n measured by SEC. The various M_v calculated by ACOMP are in good agreement with the theoretical M_n and are also less than M_w measured by SEC as expected. As shown in Figures 8 and 9 (bottom panels), the shapes of M_w vs conversion are basically linear, although they tend to deviate from the theoretical traces. These theoretical traces are based on ideal living behavior. Hence, in controlled living radical polymerizations, experimental molecular weights may be first higher than theory and then asymptotically reach the theoretical M_n, when initiation is completed.[11,36] Here, the observed deviations from linearity possibly reflect effects of significant transfer, termination, or other mechanisms. It is beyond the scope of this work to attempt such interpretations without first developing an operational quantitative approach to analysis.

ACOMP Monitoring of ATRP Activator and Deactivator Concentrations. Figure 10, from the 699 nm data, shows the semilogarithmic plot of the molar concentrations of each copper complex in the reactor vs time for experiments a and b. Previously, Cu(II) species were measured by electron spin resonance (ESR) on aliquots. The order of magnitude of the calculated concentrations of Cu^{II}Br$_2$ from ACOMP monitoring is in reasonable agreement with the published ESR values.[47]

Reaction a, with no initial Cu(II), suggests there are two phases; a rapid first one lasting 1000s after initiator injection, where an intense production of Cu(II) was observed, and a second phase in which Cu(II) concentration increases more slowly and whose slope is constant for the rest of the monitoring. With 0.04 equiv of Cu(II) vs Cu(I), however, the first phase is not observed. Such behavior is in good agreement with aforementioned results and theory.[35−37,39]

If the Cu(II) deactivator formation during the polymerization was assigned only to the termination reaction then termination rate constants were found on the order of $k_t \sim 10^{11}-10^{12}$ L·mol^{-1}·s^{-1} This range, however, is much higher than reported in the literature.[48] It appears that the signal monitored at 699 nm cannot be exclusively associated with the Cu^{II}Br$_2$ species resulting from the termination. It could be due to the outer sphere electron-transfer process,[49,50] other side reactions or air oxidation.

To check that no significant oxidation reaction of the Cu^{I}Br based complex was occurring during the ACOMP experiments, a solution of pure Cu^{I}Br/dNbpy$_2$ in THF was continuously pumped and mixed with oxygen free THF from a reservoir, and then analyzed by the detector train. It was confirmed that both RI and UV−visible

Table 5. Conversions, Molecular Weights, and Polydispersities Obtained from ACOMP and Those Obtained from SEC Analysis on an Aliquot Withdrawn at the End of the Monitoring[a]

	conversion (%)	theoretical M_n (g/mol)	M_w − ACOMP (g/mol)	M_v − ACOMP (g/mol)	M_w − SEC (g/mol)	I_p − SEC
a	32.0	7100	13 700	7700	NA	NA
b	23.5	4900	7600	5100	NA	NA
c	53.0	14 200	11 500	11 500	15 300	1.06
d	49.5	12 500	14 000	14 000	10 100	1.12
e	52.3	7000	7000	7700	10 607	1.06
f	57.3	14 500	18 400	12 600	16 800	1.06
g	44.3	28 400	37 500	28 300	34 700	1.05
h	26.5	34 000	61 500	53 000	47 683	1.12
i	47.5	12 300	11 500	15 100	15 000	1.13
j	52.5	13 400	15 200	12 100	12 000	1.10

[a] Theoretical M_n were given in function of the conversion, f, according to: $[BA]_0/[M2BP]_0 \times 128.17f$. NA: Not available.

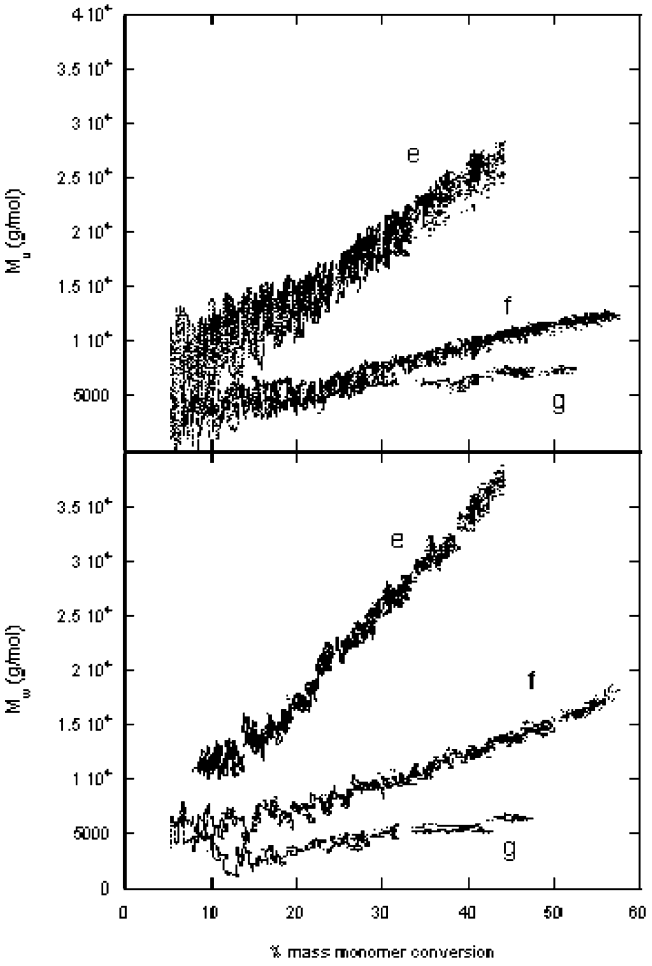

Figure 9. M_w and M_v vs mass monomer conversion in function of the targeted degree of polymerization, from top to bottom: 100 (experiment e), 200 (experiment f), and 500 (experiment g).

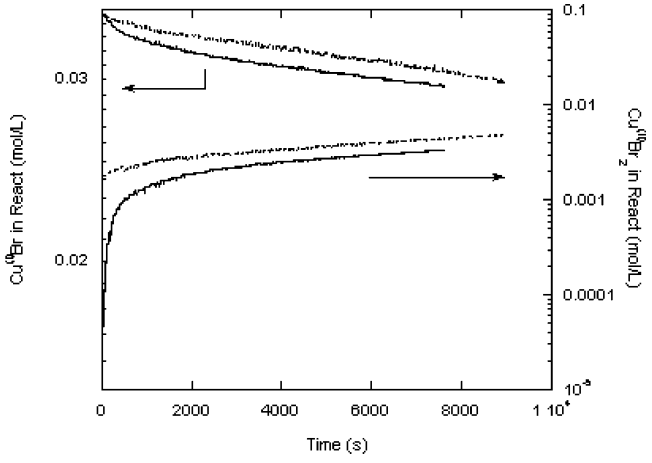

Figure 10. Semilogarithmic plot of concentrations of copper complexes vs time for experiments with variable concentration of $Cu^{II}Br_2$ added prior to initiator injection: 0 (experiment a, full line) or 0.04 equiv (experiment b, dashed line) vs $Cu^{I}Br$. t_0 is set to 0.

detectors reached their proportional value for a given percentage dilution, confirming that no significant oxidation was occurring. Afterward, the solution was deliberately oxidized by bubbling air via a peristaltic pump overnight. The solution turned green and hazy and another dilution/concentration experiment was then performed. It was found that oxidized $Cu^{I}Br/dNbpy_2$ solution has $\partial n/\partial c$ equivalent to the nonoxidized form. However, 699 nm absorption is much larger than previously measured, and is 2.5 times higher than for $Cu^{I}Br/dNbpy_2$. From these experiments, it was concluded that in the ACOMP system there is no noticeable oxidation of the Cu(I) complex and the oxidation with air could not be used to explain the continuous increase in Cu(II) in Figure 10.

Thus, more work in the UV−vis monitoring is needed to provide reliable data on termination reactions in ATRP. Efforts are currently underway to incorporate a full spectrum UV−vis diode array spectrophotometer and near infrared into ACOMP, both to meet the monitoring challenges of copolymeric and terpolymeric systems, where only limited spectral differences between comonomers exist, and to handle special problems such as copper complex monitoring.

Conclusions

Problems associated with oxidation and aggregation in ATRP were solved, allowing application of ACOMP to monitoring ATRP reactions. The data strengthen the basic understanding of ATRP kinetics and mechanisms and allow different kinetic effects and deviations from ideal behavior to be observed. A more quantitative understanding of these effects and deviations is currently being developed.

An important goal for future work is to obtain accurate concentrations of each copper species, which would permit determination of k_t. Furthermore, as ACOMP becomes more refined, and signal-to-noise is improved it may be possible to monitor, via M_w, whether there is a transition from uncontrolled to controlled behavior early in the reactions, and whether curvature of M_w vs conversion signals processes such as termination and/or chain transfer.

Current efforts focus on the application of ACOMP to controlled copolymerization kinetics involving comonomers of widely varying reactivity ratio and comonomers with significant chemical differences, but only slight spectral differences, and to quantify deviations from ideal living behavior. The stage is also set for monitoring branching reactions using polyfunctional comonomers. ACOMP should also prove useful in evaluating new homogeneous organometallic catalysts in ATRP.

Acknowledgment. Support from Arkema (Atofina), the National Science Foundation, Grants CHE 04-05627 and CTS 0124006, and the Tulane Institute for Macromolecular Engineering Science are gratefully acknowledged.

References and Notes

(1) Matyjaszewski, K., Ed. *Controlled Radical Polymerization*; ACS Symposium Series 685; American Chemical Society: Washington, DC, 1998; p 483 ff.
(2) Matyjaszewski, K., Ed.; *Controlled/Living Radical Polymerization. Progress in ATRP, NMP, and RAFT*; ACS Symposium Series 768; American Chemical Society: Washington, DC, 2000; p 484 ff.
(3) Matyjaszewski, K. Ed.; *Advances in Controlled/Living Radical Polymerization.* ACS Symposium Series 854; American Chemical Society: Washington, DC, 2003; p 688 ff.
(4) Matyjaszewski, K., Davis, T. P., Eds.; *Handbook of Radical Polymerization*; Wiley-Interscience: New York, 2002.
(5) Chiefari, J.; Rizzardo, E. In *Handbook of Radical Polymerization*; Matyjaszewski, K., Davis, T. P., Ed; Wiley-Interscience: Hoboken, NJ, 2002; pp 621−690.
(6) Hawker, C. J.; Bosman, A. W.; Harth, E. *Chem. Rev.* **2001**, *101*, 3661−3688.

(7) Kamigaito, M.; Ando, T.; Sawamoto, M. *Chem. Rev.* **2001**, *101*, 3689−3745.
(8) Matyjaszewski, K.; Xia, J. *Chem. Rev.* **2001**, *101*, 2921−2990.
(9) Wang, J.-S.; Matyjaszewski, K. *J. Am. Chem. Soc.* **1995**, *117*, 5614−5615.
(10) Fukuda, T.; Goto, A.; Ohno, K. *Macromol. Rapid Commun.* **2000**, *21* (4), 151−165.
(11) Goto, A.; Fukuda, T. *Prog. Polym. Sci.* **2004**, *29* (4), 329−385.
(12) Wang, J.-S.; Matyjaszewski, K. *Macromolecules* **1995**, *28*, 7901−7910.
(13) Matyjaszewski, K.; Patten, T. E.; Xia, J. *J. Am. Chem. Soc.* **1997**, *119*, 674−680.
(14) Wang, J.-L.; Grimaud, T.; Matyjaszewski, K. *Macromolecules* **1997**, *30*, 6507−6512.
(15) Matyjaszewski, K.; Nakagawa, Y.; Jasieczek, C. B. *Macromolecules* **1998**, *31*, 1535−1541.
(16) Davis, K. A.; Paik, H.-j.; Matyjaszewski, K. *Macromolecules* **1999**, *32*, 1767−1776.
(17) Kwark, Y.-J.; Novak, B. M. *Macromolecules* **2004**, *37*, 9395−9401.
(18) Lanzendorfer, M.; Schmalz, H.; Abetz, V.; Muller, A. H. E. *Polym. Prepr. (Am. Chem. Soc., Div. Polym. Chem.)* **2001**, *42* (1), 329−330.
(19) Florenzano, F. H.; Strelitzki, R.; Reed, W. F. *Macromolecules* **1998**, *31*, 7226−7238.
(20) Giz, A.; Catalgil-Giz, H.; Alb, A.; Brousseau, J.-L.; Reed, W. F. *Macromolecules* **2001**, *34*, 1180−1191.
(21) Çatalgil-Giz, H.; Giz, A.; Alb, A. M.; Koç, A. Ö.; Reed, W. F. *Macromolecules* **2002**, *35*, 6557−6571.
(22) Reed, W. F. *Macromolecules* **2000**, *33*, 7165−7172.
(23) Chauvin, F.; Alb, A.; Bertin, D.; Tordo, P.; Reed, W. F. *Macromol. Chem. Phys.* **2002**, *203*, 2029−2040.
(24) Mignard, E.; Leblanc, T.; Bertin, D.; Guerret, O.; Reed, W. F. *Macromolecules* **2004**, *37*, 966−975.
(25) Chambard, G.; Klumperman, B. In *Controlled/Living Radical Polymerization. Progress in ATRP, NMP, and RAFT*; ACS Symposium Series 768; Matyjaszewski, K., Ed.; American Chemical Society: Washington, DC, 2000; Vol. 768, pp 197−210.
(26) Chambard, G.; Klumperman, B.; German, A. L. *Macromolecules* **2000**, *33*, 4417−4421.
(27) Chambard, G.; Klumperman, B.; German, A. L. *Macromolecules* **2002**, *35*, 3420−3425.
(28) Pyun, J.; Jia, S.; Kowalewski, T.; Patterson, G. D.; Matyjaszewski, K. *Macromolecules* **2003**, *36*, 5094−5104.
(29) Strelitzki, R.; Reed, W. F. *J. Appl. Polym. Sci.* **1999**, *73*, 2359−2368.
(30) Norwood, D. P.; Reed, W. F. *Int. J. Polym. Anal. Charact.* **1997**, *4* (2), 99−132.
(31) Brousseau, J. L.; Çatalgil-Giz, H.; Reed, W. F. *J. Appl. Polym. Sci.* **2000**, *77*, 3259−3262.
(32) Zimm, B. H. *J. Chem. Phys.* **1948**, *16*, 1093−1099.
(33) Knuehl, B. P.; T.; Kajiwara, A.; Fischer, H.; Matyjaszewski, K. *Macromolecules* **2003**, *36*, 8291−8296.
(34) Pintauer, T.; Qiu, J.; Kickelbick, G.; Matyjaszewski, K. *Inorg. Chem.* **2001**, *40*, 2818−2824.
(35) Fischer, H. *J. Polym. Sci., Part A: Polym. Chem.* **1999**, *37*, 1885−1901.
(36) Fischer, H. *Chem. Rev.* **2001**, *101*, 3581−3610.
(37) Lutz, J.-F.; Lacroix-Desmazes, P.; Boutevin, B. *Macromol. Rapid Commun.* **2001**, *22*, 189−193.
(38) Yoshikawa, C.; Goto, A.; Fukuda, T. *Macromolecules* **2002**, *35*, 5801−5807.
(39) Shipp, D. A.; Matyjaszewski, K. *Macromolecules* **1999**, *32*, 2948−2955.
(40) Shipp, D. A.; Matyjaszewski, K. *Macromolecules* **2000**, *33*, 1553−1559.
(41) Lutz, J.-F.; Matyjaszewski, K. *Macromol. Chem. Phys.* **2002**, *203*, 1385−1395.
(42) Yoshikawa, C.; Goto, A.; Fukuda, T. *Macromolecules* **2003**, *36*, 908−912.
(43) Lutz, J.-F.; Matyjaszewski, K. *J. Polym. Sci., Part A: Polym. Chem.* **2005**, *43*, 897−910.
(44) Van Herk, A. *Macromol. Theor. Simul.* **2000**, *9*, 433−441.
(45) Barner-Kowollik, C.; Buback, M.; Egorov, M.; Fukuda, T.; Goto, A.; et al. *Prog. Polym. Sci.* **2005**, *30*, 605−687.
(46) There was a higher concentration of reactor solute in the detector train for experiments a and b and, due to the absorption by copper bromide at the multiangle laser light scattering incident wavelength of 677 nm, it was necessary to correct for the absorption in computing the Rayleigh ratio of scattered light for the computation of M_w. For the rest of the experiments, the concentration of copper bromide in the detector train gave negligible corrections to the scattering.
(47) Kajiwara, A.; Matyjaszewski, K. *Macromol. Rapid Commun.* **1998**, *19*, (6), 319−321.
(48) Beuermann, S.; Buback, M. *Prog. Polym. Sci.* **2002**, *27* (2), 191−254.
(49) Matyjaszewski, K. *Macromolecules* **1998**, *31*, 4710−4717.
(50) Matyjaszewski, K.; Woodworth, B. E. *Macromolecules* **1998**, *31*, 4718−4723.

MA050590R